LIMNOLOGY and OCEANOGRAPHY

Limnol. Oceanogr. 63, 2018, 2321–2336

doi: 10.1002/lno.10940

Resolving the long-standing puzzles about the observed Secchi depth relationships

Zhongping Lee,[1]* **Shaoling Shang**,[2]* **Keping Du**,[3] **Jianwei Wei**[1]

[1]School for the Environment, University of Massachusetts Boston, Boston, Massachusetts
[2]State Key Lab of Marine Environmental Science, Xiamen University, Xiamen, China
[3]State Key Laboratory of Remote Sensing Science, School of Geography, Beijing Normal University, Beijing, China

Abstract

Various empirical relationships have been developed in the past nine decades to link the Secchi-disk depth (Z_{SD}) with the diffuse attenuation coefficient (K_{PAR}), the euphotic zone depth (*Zeu*), and chlorophyll (Chl) concentration, where the latter two are important for the quantification and evaluation of photosynthesis in aquatic environments. There was also a classical theory regarding Secchi-disk sighting, but large gaps existed between the observations and model outcomes. These gaps have puzzled the ocean community for > 60 yr and have resulted in contradictory conclusions regarding the interpretation and usefulness of Z_{SD}. Here, we compare these measurements with data simulated based on an innovative theory and model regarding Z_{SD}, and we found remarkable agreements between theoretical predictions and these century-long observations. The results not only resolve the long-standing puzzles associated with these observations, but also unify the relationships published in the literature. In particular, the ratio of *Zeu* to Z_{SD} is found to be ~ 3.5 for all waters, which is ~ 45% greater than the consensus value of ~ 2.4 suggested in the past for clear waters. In addition, the new model validates an empirical relationship between Z_{SD} and Chl developed for global oceanic waters, thus providing strong support for using historical Z_{SD} data to study changes of phytoplankton in global oceans in the past century.

Highlights

Long-standing puzzles associated with the observed century-old dependence of the Secchi depth vs. the diffuse attenuation coefficient or the euphotic zone depth are resolved based on a new Secchi theory.

All historical observations can be unified under the new mechanistic Secchi depth model, which thus provides a strong theoretical support of an averaged relationship between the Secchi depth and chlorophyll concentration of the global oceans.

About 71% of the earth's surface is covered by water, which not only provides vital support to the life of human beings, but also modulates the climate through the coupled atmosphere-ocean system. It is imperative to have a full account of the physical and biogeochemical status of ocean waters and their spatial and temporal variations for a solid understanding of this important system. Numerous measurements have been carried out over the past centuries toward this objective, and there are a few that are unique for physical and biological oceanography. One is the measurement of water clarity, as it provides indicators of the quality of a water body and a measure of penetration of solar radiation to deeper depths, such energy is key for photosynthesis and heating at these deeper depths. Although there have been advances in optical-electronic instrumentation to measure water clarity in the 21st century, the most common approach that has been utilized over a century-long history is the measurement of Secchi-disk depth (Z_{SD}, m), invented in the 1860s by Pietro Angelo Secchi (Secchi 1864; Wernand 2010). Basically, the technique uses a white disk with a diameter of ~ 30 cm, lowered into the water, and Z_{SD} is the depth when this disk disappears from an observer at the surface. Secchi-disk depth is a direct and intuitive measure of water clarity. Because of its low cost and ease of operation in the field, there have been roughly a million Z_{SD} measurements in world oceans, lakes, and rivers in the past > 150 yr (Boyce et al. 2012, 2014), and this measurement is still routinely carried out in various surveys of aquatic environments. This extensive and long history of global Z_{SD} data are critical to evaluation of the trends of water clarity, a first order measure of water quality, of the world water bodies in the past decades to centuries (Binding et al. 2007; Olmanson et al. 2008; Shang et al. 2016). Also, changes of phytoplankton in global oceans in the past century

*Correspondence: zhongping.lee@umb.edu; slshang@xmu.edu.cn

Table 1. A list of published relationships (not exhaustive) between Z_{SD} and K_{PAR} in the past $\sim$ 90 yr. See text about calculations of MAPD.

Formula	Z_{SD} range (m)	Reference	MAPD (%)
$K_{PAR} = 1.7/Z_{SD}$	1.9–35	Poole and Atkins (1929)	21
$K_{PAR} = 1.44/Z_{SD}$	2–12	Holmes (1970)	6.3
$K_{PAR} = 1.7/Z_{SD}$	0.1–35	Idso and Gilbert (1974)	21
$K_{PAR} = 1.54/Z_{SD}$	6–46	Megard and Berman (1989)	9.8
$K_{PAR} = 1.27/Z_{SD}$	0.2–2.2	Gallegos et al. (1990)	8.4
$K_{PAR} = 1.86/Z_{SD}$	2.3–14.7	Kolengings and Edmundson (1991)	23
$K_{PAR} = 1.48/Z_{SD}^{1.16}$	1.2–5	Montes-Hugo and Álvarezborrego (2005)	14
$K_{PAR} = 1.36/Z_{SD}$	0.1–42	Lugo-Fernández et al. (2008)	6.5
$K_{PAR} = 2/Z_{SD}^{0.76}$	0.2–6	Padial and Thomaz (2008)	87
$K_{PAR} = 1.8/Z_{SD}$	0.6–4.2	Bracchini et al. (2009)	31
$K_{PAR} = 1.76/Z_{SD}^{0.85}$	1.7–7.0	Ficek and Zapadka (2010)	56
$K_{PAR} = 1.4/Z_{SD}$	0.5–2.5	Gallegos et al. (2011)	7.7
$K_{PAR} = 1.37/Z_{SD}$	0.1–2.4	Zhang et al. (2012)	10

MAPD, mean absolute percent difference.

could be inferred from Z_{SD} data (Boyce et al. 2010; Boyce and Worm 2015).

In addition, because natural waters, especially those of the open ocean, are transparent to light in the visible domain, it is important to quantify this solar energy at depths in order to evaluate the contribution to photosynthesis and heating in the water column. In modern ocean optics, the attenuation of visible solar radiation is calculated using the diffuse attenuation coefficient (Kirk 1994; Mobley 1994) in its wavelength resolved ($K_d(\lambda)$, m^{-1}) or wavelength integrated forms (K_{PAR}, m^{-1}), where the latter is also commonly termed as the diffuse attenuation coefficient of the photosynthetically available radiation (PAR). Because there was historically no or limited equipment to measure the vertical profile of solar radiation in water that is required to calculate K_d or K_{PAR} values, it would be desirable to convert the measurements of Z_{SD} to K_d or K_{PAR}, especially for historical measurements made before modern instrumentation was available. Therefore, in the past decades, a number of empirical relationships have been developed between Z_{SD} and K_{PAR} or between Z_{SD} and K_d based on measurements in various water bodies. These relationships show great consistency in general dependence for waters from open ocean to inland turbid lakes, but also show variations in empirical constants. Specifically, from concurrent measurements of Z_{SD} and K_{PAR} at various regions by various groups in the past $\sim$ 90 yr (Poole and Atkins 1929; Holmes 1970; Megard and Berman 1989; Zhang et al. 2012), it is found empirically that there is a general relationship as

$$K_{PAR} = \frac{\alpha}{Z_{SD}}. \tag{1}$$

Because such a dependence has been observed by numerous groups for a wide range of waters, the relationship between Z_{SD} and K_{PAR} cannot be viewed as accidental, although the model coefficient α has been reported in a range of $\sim$ 1.3–2 rather than a universal constant (*see* Table 1). There have been inconclusive debates in the past decades on the appropriate α value for use in this relationship (Holmes 1970; Boivin et al. 1986; Padial and Thomaz 2008).

On the other hand, euphotic zone depth (*Zeu*, m), commonly and practically defined as the depth where PAR(*Zeu*) is 1% of PAR(0), is an important bio-optical property for the evaluation of water-column primary production and the biological pump (Platt et al. 1991; Sathyendranath and Platt 1995; Behrenfeld and Falkowski 1997*b*; Falkowski 1998). Because there are times (especially in the earlier days of ocean observations) where no instrument is available to measure *Zeu*, it is desirable to convert Z_{SD} to *Zeu*, and an empirical relationship was also developed based on field measurements

$$Zeu \approx \beta Z_{SD}. \tag{2}$$

The value of β has been reported in a range of $\sim$ 1–10 in the literature (Koenings and Edmundson 1991; Luhtala and Tolvanen 2013), with a consensus value of 2.4 suggested for clear waters. Again, the appropriate β value for this conversion has been vague and inconclusive.

More importantly, because the concentration of chlorophyll (Chl, mg/m^3) is an important indicator of eutrophication, and a parameter in traditional models for primary production (Platt 1986; Behrenfeld and Falkowski 1997*a*), there have also been numerous attempts to empirically convert Z_{SD} to Chl (Carlson 1977; Lewis et al. 1988; Falkowski and Wilson 1992), where an even wider range of formulations and empirical coefficients have been presented in the literature.

There were also attempts to explain the observed relationships between Z_{SD} and K_{PAR}, *Zeu* or Chl based on the theory of visual optics or Secchi theory (Duntley 1952; Preisendorfer 1986), but results were far from conclusive or successful (Graham 1966; Bukata et al. 1988; Davies-Colley and Vant 1988; Morel et al. 2007*b*; Doron et al. 2011; Gallegos et al. 2011; Effler et al. 2017). In particular, as articulated in Preisendorfer (1986), the observed nearly "universal" relationship (Holmes 1970) between Z_{SD} and K_{PAR} actually could not be explained with the classical Secchi theory. This discrepancy between theory and observations has puzzled the community for decades.

A recent study (Lee et al. 2015*a*) found that this classical Secchi theory does not match the process of our eye and brain in deciding the sighting of a Secchi disk in water, and subsequently, a new theory and model have been developed to explain Z_{SD}. This new theory was verified with measurements from open ocean to inland waters. With this breakthrough, we here use numerical simulations to compare theoretical predictions with historical observations between Z_{SD} and K_{PAR}/Chl/*Zeu*, with an attempt to resolve the long-standing puzzles associated with the historical observations and to unify all empirical relationships developed in the past $\sim$ 90 yr. The results from this effort not only provide sound interpretations of the observed data and relationships in the past century, but also establish a solid base to confidently and accurately convert Z_{SD} data to other useful optical properties.

Brief summary of the theoretical Secchi models

Following the law of contrast reduction in the atmosphere (Middleton 1957) and based on radiative transfer, Duntley (1952) developed a theoretical model between Z_{SD} (without consideration of the air-sea surface effect) and water's optical properties as

$$Z_{SD}=\frac{1}{K_d(\nu)+c(\nu)}\ln\left(\frac{1}{C_t}\frac{R_T(\nu)-R_w(\nu)}{R_w(\nu)}\right). \tag{3a}$$

Here, K_d, c (m^{-1}) and R_w are the diffuse attenuation coefficient of downwelling irradiance, beam attenuation coefficient, and diffuse reflectance of the water body, respectively. Letter "ν" represents all the values are weighted by the response function of a human eye in the visible domain. R_T is the reflectance of a white Secchi disk, which is around 0.85 (Tyler 1968). C_t is the threshold of eye detection (Blackwell 1946), commonly considered between $\sim$ 0.005 and 0.02 (Tyler 1968; Hou et al. 2007). For simple description, the above equation is usually simplified as

$$Z_{SD}=\frac{\Gamma}{K_d(\nu)+c(\nu)}, \tag{3b}$$

with parameter Γ reported in a range of $\sim$ 5–10 (Gordon and Wouters 1978; Preisendorfer 1986). This model was subsequently echoed in Tyler (1968), Preisendorfer (1986), Zaneveld and Pegau (2003), Levin and Radomyslskaya (2012), and Aas et al. (2014) and has been followed by the community in the past 60+ years to theoretically interpret Z_{SD} data. A few later models (e.g., Preisendorfer 1986; Levin and Radomyslskaya 2012) included a term to explicitly consider the air–sea surface effects, but that term was generally imbedded in the parameter Γ in most of such models.

Clearly, because in general K_d and c are two independent optical properties, and $c \gg K_d$ for most natural waters in the visible domain, the inconsistency between the theory (Eq. 3) and observations (Eq. 1) has puzzled the community since the 1950s. Recently, He et al. (2017) presented a radiative-transfer–based model where Z_{SD} is linked to the absorption and backscattering coefficients at 443 nm, but the physics behind this model is vague, which cannot explain the observed relationships between Z_{SD} and K_{PAR}. On the other hand, Lee et al. (2015*a*) questioned the validity of Eq. 3 as the theoretical base to interpret and model Z_{SD} and pointed out that there are serious shortcomings or mistakes in the derivation of Eq. 3. They include

1. A Secchi disk was treated as a point to a human eye in this classical theory. However, because of the super angular resolution of our eyes, a 30-cm disk with a distance of tens of meters is still very large to our eyes. Consequently, a key assumption employed in the derivation of Eq. 3 is not held (Lee et al. 2015*a*), which then disproves the derivation of Eq. 3.
2. The decision of sighting a Secchi disk in water by the human eye–brain system is based on information in water's transparent window (at the wavelength of maximum transmittance) (Megard and Berman 1989; Aas et al. 2014; Lee et al. 2015*a*), not the full visible spectrum as depicted in the classical theory or at a fixed wavelength (He et al. 2017). This is further supported with experiments in blue and green waters (Aas et al. 2014; Lee et al. 2017).
3. The decision on detection of human eyes is based on absolute difference in radiance or reflectance (Blackwell 1946; Bartleson and Breneman 1967) rather than on relative difference (the ratio of (R_t–R_w) to R_w) as employed in the classical theory (Duntley 1952; Preisendorfer 1986). As discussed detailed in Lee et al. (2015*a*), the evaluation of relative difference is a good measure of the sharpness of an object, but it does not match the concept of "brightness constancy" in visual detection (Bartleson and Breneman 1967; Freeman 1967). Further, the use of such a ratio contributes to the large variation of Γ in the classical Z_{SD} model because R_w change a lot from water to water (Gordon and Wouters 1978; Preisendorfer 1986).

To overcome the abovementioned mistakes or shortcomings, a new theory and model regarding Z_{SD} have been proposed (Lee et al. 2015*a*), where Z_{SD} is approximated as

$$Z_{SD} = \frac{1}{2.5\ K_d^{tr}} \ln\left(\frac{|0.14 - R_{rs}^{pc}|}{C_t^r}\right). \tag{4}$$

Here, K_d^{tr} is K_d at the transparent window of a water body, while R_{rs}^{pc} is the value of remote sensing reflectance (R_{rs}, sr^{-1}) at the perceived color of the water body when a Secchi disk disappears. C_t^r is the contrast threshold of detection, which is around 0.013 sr^{-1} based on measurements of Blackwell (1946). In particular, as detailed in Lee et al. (2015*a*), the contrast employed in the new Secchi theory is the ratio of absolute difference of radiance to incident light, which is constant with the concept of "brightness constancy."

Further, field measurements from a wide range of environments indicate that the logarithm term on the right side of Eq. 4 is within a narrow range (2.38 ± 0.03), which suggests that Z_{SD} generally follows (eq. 36 of Lee et al. 2015*a*)

$$Z_{SD} \approx \frac{1}{K_d^{tr}}. \tag{5}$$

Clearly, there are significant differences between the two theoretical models for Z_{SD}. In particular, K_d is in general a function of the absorption (a, m^{-1}) and backscattering (b_b, m^{-1}) coefficients (Gordon and Wouters 1989; Lee et al. 2005*b*); while c is the sum of a, b_b, and b_f (the forward scattering coefficient). Because b_f is independent of b_b and b_f is, in general, 50X or more larger than b_b, so c can be many times larger than K_d in the visible domain (also *see* Preisendorfer 1986, Davies-Colley and Vant 1988). Thus, in the classical model, Z_{SD} is generally governed by c, with K_d playing a minor role. In contrast, Z_{SD} is governed by K_d in the transparent window of a water body in the new theory and model, where there is no association with the beam attenuation coefficient (c).

Although the new model was verified using concurrent measurements of Z_{SD} and remote sensing reflectance (Lee et al. 2015*a*), it is still important, both theoretically and practically, to determine if the new model indeed provides a sound interpretation of Z_{SD} observations and then resolves puzzles associated with the historical relationships that date back over nearly 90 yr.

Data and methods

Following the approach adopted in IOCCG Report 5 (IOCCG-OCAG 2003; IOCCG 2006), a dataset of wide range of IOPs was synthesized, and K_d and K_{PAR} were further calculated from profiles of solar radiation simulated with Hydrolight (Mobley and Sundman 2013). Briefly, for inclusive IOPs spectra matching field observations, as articulated in *Models, parameters, and approaches that are used to generate wide range of absorption and backscattering spectra* (IOCCG-OCAG 2003), the absorption (a) and backscattering (b_b) coefficients were modeled as (Mobley 1994):

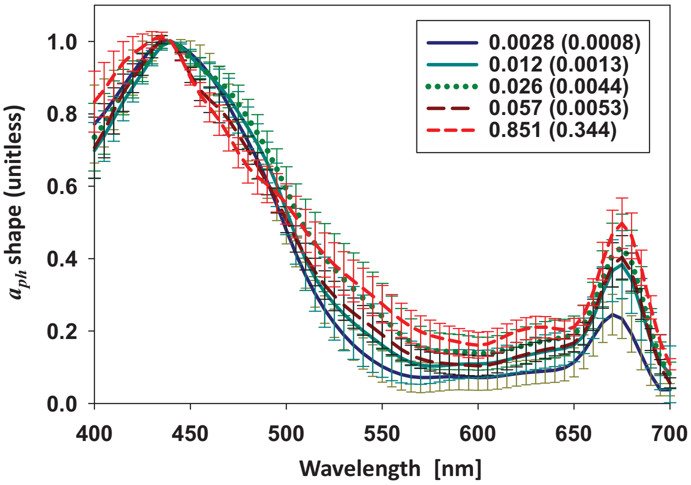

Fig. 1. Examples of $a_{ph}(\lambda)$ spectral shapes used in the generation of the synthesized data. They are obtained from SeaBASS and measurements from cyanobacteria bloom waters (Mishra et al. 2013). Values in the box are corresponding average $a_{ph}(440)$ (m^{-1}) and standard deviation of each a_{ph} group.

$$a(\lambda) = a_w(\lambda) + a_{ph}(\lambda) + a_{dm}(\lambda) + a_g(\lambda) \tag{6a}$$

$$b_b(\lambda) = b_{bw}(\lambda) + b_{bph}(\lambda) + b_{bdm}(\lambda) \tag{6b}$$

Here, subscripts "w, ph, dm, g" represent pure seawater, phytoplankton pigments, detritus and minerals, and gelbstoff (or colored dissolved organic matter, CDOM). The spectral range is 400–700 nm with a step of 5 nm.

Values of $a_w(\lambda)$ were taken from the combinations of Sogandares and Fry (1997), Lee et al. (2015*b*), and Pope and Fry (1997); values of b_{bw} were from Zhang et al. (2009). As detailed in (IOCCG-OCAG 2003), a core aspect of the generation of the wide range of IOPs lies in the use of a_{ph} as a key free variable, with other optically active properties treated as free variables, but constrained in a range in relation to a_{ph} (IOCCG-OCAG 2003).

A total of 720 $a_{ph}(\lambda)$ spectra representing oceanic to phytoplankton bloom waters were selected from ~ 4000 measurements submitted to SeaBASS. The 720 a_{ph} spectra (covering an $a_{ph}(440)$ range of ~ 0.0014–39.0 m^{-1}) were divided into 12 groups, with each group covering a small range of $a_{ph}(440)$. Figure 1 shows the general a_{ph} spectral shapes of a few of these groups, where the natural variation of the spectral shapes is retained in this synthesized dataset. Subsequently, as described in detail in IOCCG-OCAG (2003), spectra of a_{dm}, a_g, b_{bph}, and b_{bdm} were modeled based on values of $a_{ph}(440)$, where random values of a_{dm}, a_g, b_{bph}, and b_{bdm} were synthesized for a given $a_{ph}(440)$ value. The scattering phase function of phytoplankton was a Fournier and Forand function (Fournier and Forand 1994) with a backscattering ratio of 1%, while the scattering phase function of detritus/sediment was the averaged Petzold phase function (Petzold 1972; Mobley 1994) with a backscattering ratio of 1.83%. Because the variations of IOPs were not determined by Chl alone, we may call this dataset Non-Case-1 data, where the ratio of $(a_{dm}+a_g)/a_{ph}$ at 440 nm is in a range of ~ 0.4–6.5 (2.8 ± 1.4), and the ratio of $b_b/(a+b_b)$ at 440 nm is in a range of ~ 0.001–0.33 (0.075 ± 0.071).

Further, sun was set at 30° from zenith, wind was set as 5 m/s, while downwelling irradiance just above the surface was modeled using RADTRAN (Gregg and Carder 1990). Depth was set from 0 m to 200 m with 21 layers for these simulations.

With the simulated profiles of PAR (in Ein/s/m^2) and spectral downwelling irradiance (E_d, W/m^2/nm), K_{PAR} and spectral K_d were calculated, respectively, for each set of IOPs, using,

$$K_{PAR}=\frac{1}{z}\ln\left(\frac{PAR(0)}{PAR(z)}\right), \tag{7}$$

$$K_d(\lambda)=\frac{1}{z}\ln\left(\frac{E_d(\lambda,0)}{E_d(\lambda,z)}\right). \tag{8}$$

Because K_{PAR} is highly depth dependent (Lee 2009), three sets of K_{PAR} were calculated to represent the averages between surface to 30% (represented as $K_{PAR}(30\%)$), to 10% ($K_{PAR}(10\%)$), and to 1% ($K_{PAR}(1\%)$), respectively. K_d is a weak function of depth (Mobley 1994; McCormick 1995), therefore, similarly as for the calculation of K_{PAR}, three sets of K_d for depth ranges between surface to 30% (represented as $K_d(\lambda,30\%)$), to 10% ($K_d(\lambda,10\%)$), and to 1% ($K_d(\lambda,1\%)$) were calculated, respectively. Further, the value of K_d^{tr} for each set of IOPs was taken as the minimum $K_d(\lambda,10\%)$ within the 400–700 nm spectral range, and thisK_d^{tr} was converted to Z_{SD} following Eq. 5. Thus, we obtained a set of theoretical K_{PAR} and Z_{SD} (represented as Z_{SD}^{new} in the following) for this synthetic dataset.

Results and discussion

Z_{SD} vs. K_{PAR}

The K_{PAR} vs. Z_{SD}^{new} dependence was first compared with published data in the literature (Poole and Atkins 1929, Holmes 1970, Davies-Colley and Vant 1988, Megard and Berman 1989, Gallegos et al. 1990) and is presented in Fig. 2. For Z_{SD} in a range of ~ 0.2–46 m and collected by different groups from 1929 to 1990, with different instruments for light intensity, and covering waters from oligotrophic ocean waters to turbid inland waters, it is found, at least visually, that the K_{PAR} vs. Z_{SD} dependence from field measurements matches the theoretical K_{PAR} vs. Z_{SD}^{new} extremely well (*see* Fig. 2). This match echoes the claim that the observed K_{PAR} vs. Z_{SD} dependence is "universal" (Holmes 1970) and well supported by the new theory regarding Secchi-disk observations, although not all measurements fall exactly on the theoretical predictions (more discussions are followed regarding these deviations).

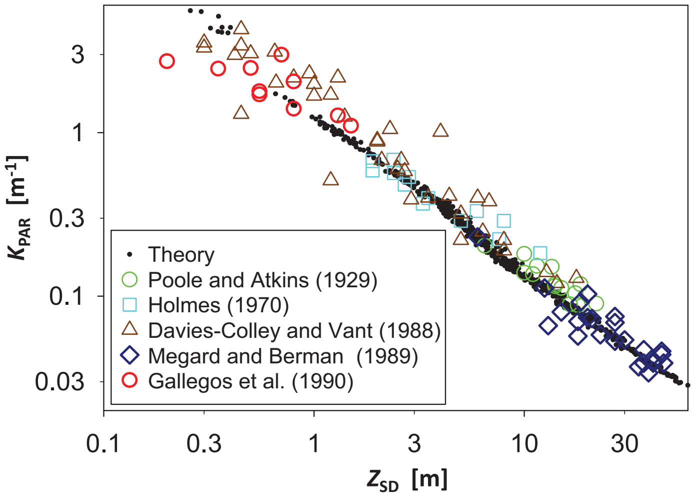

Fig. 2. A scatterplot between Z_{SD} and K_{PAR} with data from simulations and published in the literature. The simulated Z_{SD} for this Non-Case-1 data followed the new Secchi theory (Eqs. 4 and 5), and $K_{PAR}(10\%)$ is used to represent K_{PAR} of the simulated data.

We further quantitatively evaluated the average dependences by measuring the accuracy of estimated K_{PAR} derived from the theoretical Z_{SD} values using the published relationships (*see* Table 1). The underlying assumptions are: If the new theory and model (Eqs. 4, 5) regarding Secchi depth are sound and robust, then the Z_{SD} values can be used to convert to K_{PAR} using an observed K_{PAR}–Z_{SD} relationship, and the converted K_{PAR} should approximate those calculated using Hydrolight. The mean absolute percent difference (MAPD) between the two sets of K_{PAR} values is calculated to measure the accuracy of this estimation

$$MAPD=\frac{1}{n}\sum_{n}\frac{|K_{PAR}^{est}-K_{PAR}^{HL}|}{K_{PAR}^{HL}}\times 100\%, \tag{9}$$

with K_{PAR}^{HL} for values from Hydrolight simulations, while K_{PAR}^{est} for values estimated from Z_{SD}^{new} using the published relationships. Note that because K_{PAR} is depth dependent, here K_{PAR}^{HL} is the value of K_{PAR} (10%). The MAPD values for 13 relationships published in the past ~ 90 yr are also included in Table 1. For illustration purposes, Fig. 3 presents scatter plots of K_{PAR}^{HL} vs. K_{PAR}^{est} for a few of the 13 relationships.

Values of MAPD varied in a range of ~ 6–81% for the 13 relationships evaluated (Table 1), with 10 out of 13 relationships having MAPD less than ~ 23%, and six out of 13 having MAPD less than ~ 10%. Considering there are uncertainties or errors associated with field measurements, especially on the fundamental nature of K_{PAR} (*see* Lee 2009 and below for detailed discussions), the less than ~ 23% difference between K_{PAR}^{HL} and K_{PAR}^{est} for Z_{SD} in a range of ~ 0.2–46 m indicates an excellent consistency between the new theory and the historical observations of the past ~ 90 yr.

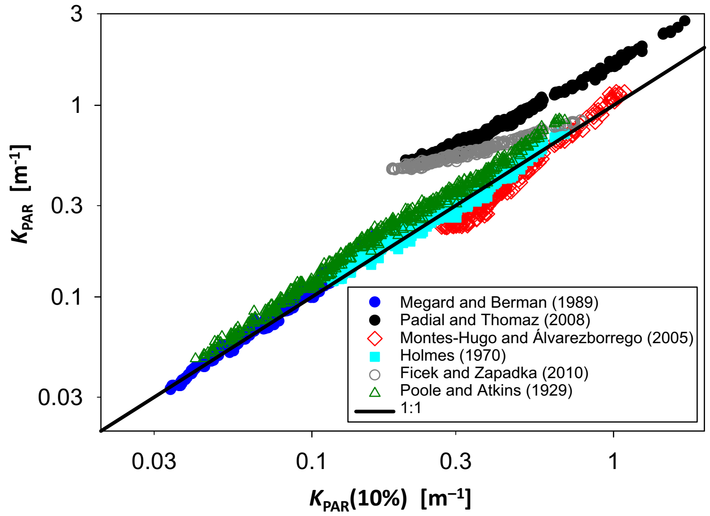

Fig. 3. Examples of Hydrolight K_{PAR}(10%) compared with K_{PAR} derived from simulated Z_{SD} using published Z_{SD}–K_{PAR} relationships.

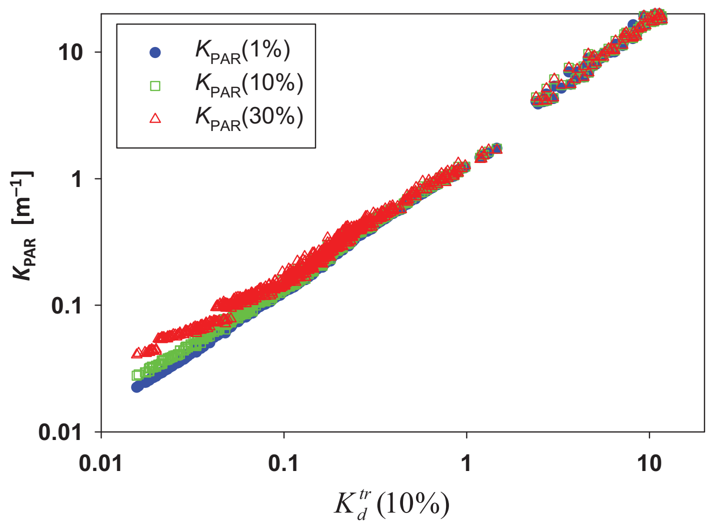

Fig. 4. Relationship between K_{PAR} and K_d^{tr} of the simulated dataset.

Another way to evaluate the historical observations with the numerical simulations is to compare K_{PAR} with K_d^{tr} (*see* Fig. 4). It appears that the two are extremely correlated ($R^2 > 0.99$) for the wide range of optical properties (K_{PAR} (10%) in a range of $\sim$ 0.03–25 m^{-1}), although there are different slopes for K_{PAR} calculated with different depth ranges. One reason for this high R^2 value is the wide ranges of K_{PAR} with K_d^{tr}, but the key reason is that fundamentally the optically varying components (a_{ph}, a_{dm}, a_g, b_{bph}, and b_{bdm}) of natural waters are spectrally wide, therefore a variation in the shorter wavelengths (say 400–500 nm) that changes the value of K_d^{tr}, will also change the value of K_{PAR}.

Further we calculated the ratio (rK2K) of K_{PAR} to K_d^{tr}, with averages and standard deviations presented in Table 2. Depending on the depth ranges used for the calculation of K_{PAR} and K_d, there are different ratios of rK2K (*see* Table 2). For the K_{PAR} and K_d calculated here, it is found the averages of rK2K ranged from 1.32 to 1.69 (larger values for shallower depth ranges), with an overall average as 1.48 ($\pm$0.22) for the six combinations.

Therefore Eq. 5 can be re-written as

$$Z_{SD} \approx \frac{1.48}{K_{PAR}}. \tag{10}$$

This dependence is remarkably consistent with the reported relationships in the literature published in the past $\sim$ 90 yr from measurements in a wide range of environments. In

Table 2. Average ratios and standard deviations of K_{PAR} to K_d^{tr} (rK2K) for data from Hydrolight simulations.

	K_{PAR}(1%)	K_{PAR}(10%)	K_{PAR}(30%)
To K_d^{tr}(1%)	1.32 ± 0.09	1.43 ± 0.12	1.63 ± 0.27
To K_d^{tr}(10%)	1.36 ± 0.09	1.48 ± 0.12	1.69 ± 0.28

particular, Walker (1980) obtained an average α value as 1.45 from a wide range of measurements. This consistency with independent approaches and analyses further validates the new theoretical model presented by Eqs. 4, 5.

For individual measurements of K_{PAR} and Z_{SD}, Weidemann and Bannister (1986) reported a range of α as $\sim$ 1.0–1.9, while Koenings and Edmundson (1991) reported a much wider range as $\sim$ 1.1–3.8. Because each individual measurement in the field could be associated with various levels of errors or uncertainties that require detailed information to analyze, we here omit discussions on the individual values, focusing rather on the average (the model constant presented in Table 1) where such measurement-related errors could be minimized.

There are a range of factors contributing to the variations of α (including the reported averages) and the nonzero MAPD. One is the uncertainty associated with Z_{SD} measurements, which is generally viewed as $\sim$ 10–15%. The accuracy of K_{PAR} depends on robust and accurate measurements of PAR(z) in the field, but uncertainties or errors, which can sometimes be very large, are not uncommon in field measurements. The sources for these uncertainties include imperfect calibration of the PAR sensor (note that, there is a change in the color of solar radiation with increasing depth), ship perturbation (Gordon and Wouters 1985) (PAR was usually measured by the side of a survey boat historically), wave focusing/defocusing (Stramski and Legendre 1992; Wei et al. 2014), and stratified water column, and so forth. These uncertainties or errors will contribute to variations among the α values obtained from each station. A key and systematic source of uncertainty or error in the historical studies, however, is actually the implicit assumption that K_{PAR} is a constant vertically, thus K_{PAR} obtained from any depth range could be considered, implicitly, representative of that of the water column, or that between the surface and Z_{SD}. But, as articulated in Lee (2009), even if PAR is measured perfectly, K_{PAR} itself is ambiguous and comparison of K_{PAR} values is like an "apples and oranges" comparison.

Commonly, K_{PAR} in all studies were calculated as (Holmes 1970; Idso and Gilbert 1974; Gallegos et al. 1990; Padial and Thomaz 2008)

$$K_{PAR} = \frac{1}{z_2 - z_1} \ln\left(\frac{PAR(z_1)}{PAR(z_2)}\right), \tag{11a}$$

or as the slope between ln(PAR(z)) and z,

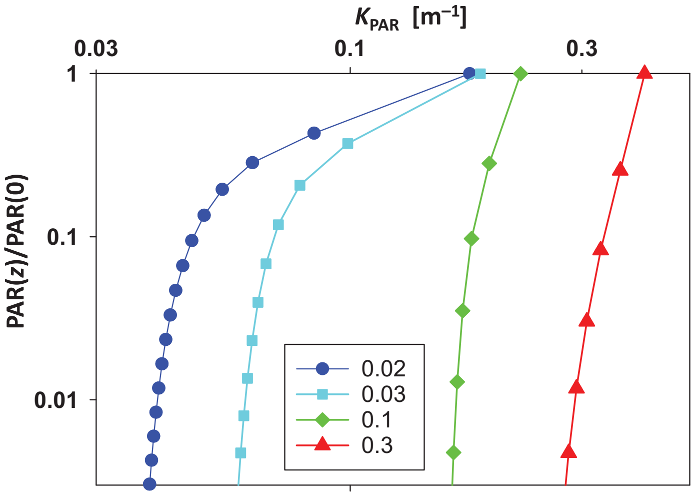

Fig. 5. Examples of vertical profiles of K_{PAR}. Values in the box are a(490) (m^{-1}).

$$\ln(PAR(z)) = \ln(PAR(0)) - K_{PAR} \times z. \tag{11b}$$

However, as indicated in Megard and Berman (1989) and discussed in detail in Lee (2009), values of K_{PAR} are highly depth dependent even for homogeneous waters. Further, this depth variation of K_{PAR} depends on water properties. Figure 5 presents examples of depth varying K_{PAR} for four different waters, where K_{PAR} in the upper layer can be approximately three times larger than K_{PAR} in deeper depths for oligotrophic waters (also *see* fig. 1b of Lee et al. 2014). Therefore, there are inherent ambiguities and uncertainties when comparing K_{PAR} values from one study to another if the range of depth is not the same or not specified, and this uncertainty will propagate to the published average α values when Z_{SD} is related to K_{PAR}. This will further contribute to the MAPD values when comparing theoretical K_{PAR} (where K_{PAR} is clearly defined or constrained) to estimated K_{PAR} using published relationships (where K_{PAR} was not well defined or constrained).

This ambiguity of K_{PAR} and the vertical patterns for different waters are the fundamental reasons contributing to the puzzle or debate related to the different α values obtained from field measurements, but these reasons have been generally overlooked in the past decades. For example, K_{PAR} in Padial and Thomaz (2008) was determined for a depth range between 0 m and 0.2 m, which is a layer where K_{PAR} is generally much higher than K_{PAR} of deeper depth ranges (*see* Fig. 5). On the other hand, most of the Z_{SD} values of the waters surveyed by Padial and Thomaz (2008) were in a range of $\sim$ 1–6 m. Thus, the significantly higher K_{PAR} in the surface layer (0 m and 0.2 m) did not represent the K_{PAR} for the depth range between the surface and Z_{SD}, which then lead to a much larger α value and then much higher MAPD ($\sim$ 81%) when using their relationship to evaluate K_{PAR} (10%) simulated by Hydrolight.

This ambiguity is also due to the depth variation of K_{PAR} that resulted in a smaller α value (1.44) in Megard and Berman (1989) compared to the 1.7 reported in Poole and Atkins (1929), where Megard and Berman (1989) used K_{PAR} from deeper layers (smaller K_{PAR}), rather than a K_{PAR} from the surface to some depth (larger K_{PAR}) as in Poole and Atkins (1929). Also, smaller α values were obtained when K_{PAR} was calculated from surface PAR to a depth close to 1% PAR (e.g., Holmes 1970, Gallegos et al. 1990, Zhang et al. 2012), as these K_{PAR} are always smaller than K_{PAR} calculated from layers above it (*see* Fig. 5).

Furthermore, α values of clear waters were found to be larger than that of turbid waters (Holmes 1970; Koenings and Edmundson 1991), and this "puzzle" was vaguely explained with turbidity (Davies-Colley and Vant 1988; Koenings and Edmundson 1991). Actually, this clear vs. turbid water contrast of α values is again due to the nature of K_{PAR} vertical patterns. As presented in Fig. 5, because K_{PAR} of the surface layer is significantly larger than that of deeper layers for clearer waters, and the surface K_{PAR} was usually used to represent K_{PAR} of the entire water column, consequently a larger α value would be derived from field measurements for clearer waters. However, this depth variation of K_{PAR} reduces with the increase of turbidity (or shallower Z_{SD}) (*see* Fig. 5). Therefore, K_{PAR} of the surface layer is more representative of K_{PAR} of the entire water column for more turbid waters, where consequently smaller α values (which are also more consistent with that predicted by the new Secchi theory) were obtained. This is evidenced in Holmes (1970), Davies-Colley and Vant (1988), and Koenings and Edmundson (1991), where larger α values were found for waters with deeper Z_{SD} (clear waters), and smaller α values for waters with shallower Z_{SD} (turbid waters).

We do see contradictory reports from these field measurements though. For instance, Idso and Gilbert (1974) calculated K_{PAR} for a depth range of 0.02–0.2 m and found α on average about 1.7, but the Z_{SD} range is similar to that reported in Poole and Atkins (1929). Based on Hydrolight simulations and those of Padial and Thomaz (2008), the α values in Idso and Gilbert (1974) should be much higher than that reported in Poole and Atkins (1929). On the other hand, Koenings and Edmundson (1991) and Bracchini et al. (2009) obtained much larger α than that reported in Holmes (1970), where by description, Koenings and Edmundson (1991) and Bracchini et al. (2009) calculated K_{PAR} using depths much deeper than those in Idso and Gilbert (1974) and Padial and Thomaz (2008). These unusual observations, however, are not common in the literature. In general, all the reported average α values are within a range of $\sim$ 1.4–1.9, consistent with that predicted by the new Secchi theory and model.

In conclusion, although theoretically a general dependency between Z_{SD} and K_{PAR} (Eq. 1) is found rooted in Secchi theory (Eqs. 4, 5, 10), but discrepancies exist when applying to field data due to the following: (1) K_{PAR} is inherently ambiguous; (2) the determination of K_{PAR} values from field measurements followed no standard protocol within or among different groups, thus two K_{PAR} quantities are not actually the "same" or comparable; and (3) K_d^{tr}(that determines Z_{SD}) may not be exactly determined by K_{PAR} due to different mechanisms, therefore variations in α values would be expected from field-measured Z_{SD} and K_{PAR}. This ambiguity in K_{PAR} determined from field measurements may be the main factor contributing to the puzzle and debate in the past decades about which α value is more appropriate to use.

The fundamental difference between K_d^{tr} and K_{PAR} also explains the puzzling much higher α value that appeared for stained lake waters observed in Koenings and Edmundson (1991). This special case is likely due to the fact that this stain water has a very high K_{PAR} to K_d^{tr} ratio, cases that also exist in the simulated data (range of rK2K is $\sim$ 1.2–2.1). For instance, for waters with a high amount of CDOM and nearly no particles, K_{PAR} in the surface layer can be approximately three times of K_d^{tr} due to the exponential decrease of a_g with wavelength. Since Z_{SD} is determined by photons in the transparent window $\left(K_d^{tr}\right)$ rather than photons of the entire visible domain, the use of K_{PAR} for this Z_{SD} will result in an α value even larger than that of clear waters as shown in Koenings and Edmundson (1991).

There were also empirical models to describe Z_{SD} as a function of $K_d(490)$ and described as (Suresh et al. 2006),

$$Z_{SD} \approx \frac{1.45}{K_d(490)}. \tag{12}$$

Fundamentally, $K_d(490)$ is always $\geq K_d^{tr}$; and the ratio of $K_d(490)$ to K_d^{tr} is found generally in a range of 1.0–4.0 in the simulated dataset. Thus, based on Eq. 5, Z_{SD} estimated using Eq. 12 is only reliable for waters where $K_d(490)$ is $\sim 1.45K_d^{tr}$. Z_{SD} will be overestimated by about 45% when $K_d(490)$ approximates K_d^{tr} (i.e., 490 nm is the transparent window) and will be underestimated significantly when $K_d(490)$ is much greater than K_d^{tr}, and this underestimation could happen in both oceanic blue waters or coastal productive waters.

The classical model

Although it has been pointed out that the classical model for Secchi-disk depth (Eq. 3) could not be derived from radiative transfer (Lee et al. 2015*a*), out of curiosity and to caution future applications of this classical model, we also estimated Z_{SD} of the synthetic data using the latest approximations of this model. To apply Eq. 3 for Z_{SD} estimation, it requires knowing both Γ and $K_d(v) + c(v)$. Following earlier practices (Gordon and Wouters 1978), Doron et al. (2011) proposed to calculate Γ as

$$\Gamma = \ln\left(\frac{0.82 - R_W(490)}{R_W(490)} \Big/ 0.02\right). \tag{13}$$

Because values of $R_w(490)$ are available from Hydrolight simulations, it is easy to obtain values of Γ of the synthetic data, and it is found in a range of ~ 6–10, consistent with that reported in the literature. This echoes that an uncertainty will be introduced in the estimation of Z_{SD} using the classical model if a constant Γ value is used (Gordon and Wouters 1978).

Based on bio-optical modeling, Doron et al. (2011, 2007) found that $K_d(\nu) + c(\nu)$ can be described as a function of $K_d(490) + c(490)$,

$$K_d(\nu)+c(\nu)=0.0989\,X^2+0.8879\,X+0.0467. \tag{14}$$

where, X is $K_d(490) + c(490)$. Because $c(490)$ was synthesized and $K_d(490)$ was calculated from Hydrolight simulations, it is thus straightforward to estimate Z_{SD} (termed as Z_{SD}^{old} in the following to represent these results) of the synthetic data following the classic model (Eq. 3a). (Note that, there is a typo of this equation in Doron et al. (2011, 2007), where there should be no "–" before "0.0467.")

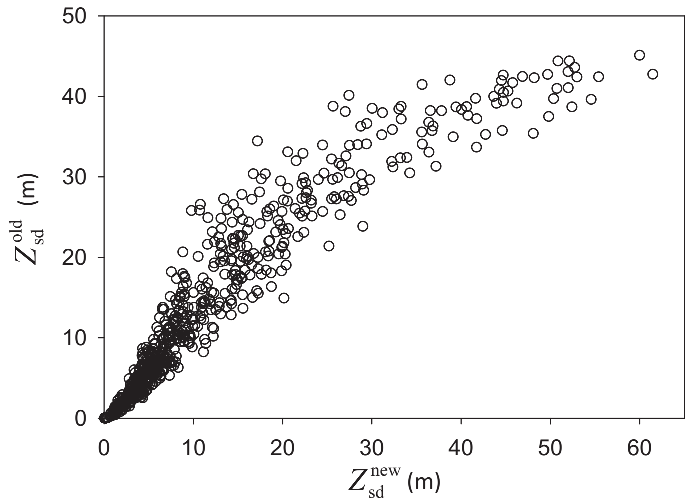

Fig. 6. A comparison between Z_{SD} estimated with the new Secchi theory vs. Z_{SD} estimated with the classical Secchi theory for the synthesized IOPs.

Figure 6 compares Z_{SD}^{old} with Z_{SD}^{new} for the synthesized IOPs. There are obvious differences ($R^2 = 0.89$) between the two estimates, where the range of Z_{SD}^{old} is ~ 0.0004–45 m, while Z_{SD}^{new} is ~ 0.05–62 m. Further, as in the above practice to evaluate Z_{SD}^{new}, these Z_{SD}^{old} values were converted to K_{PAR} using the published relationships, and then compared to that from Hydrolight simulations (K_{PAR} (10%)), with sample results presented in Fig. 7. As expected, there are large differences (in a range of ~ 29–131% for the relationships published in Table 1) between Z_{SD}^{old}-converted K_{PAR} and K_{PAR}^{HL}. These results further indicate a gap or inconsistency between the classical Z_{SD} model and observations in the field. Such gaps were actually revealed in the past (Bukata et al. 1988; Davies-Colley and Vant 1988; Gallegos et al. 2011; Aas et al. 2014; Effler et al. 2017), where no "universal" relationships were observed between Z_{SD} and $\Gamma/(K_d + c)$. But these observed deviations were commonly attributed to environmental factors (such as the variation of Γ and/or particle phase functions) in the past decades, rather than the theoretical derivation itself to reach Eq. 3.

Z_{SD} vs. Chl

Researchers have long wished to convert the large number of historical collections of Z_{SD} to Chl concentration, as a way to study eutrophication (Carlson 1977) and the change of global phytoplankton (Lewis et al. 1988; Falkowski and Wilson 1992). Subsequently, many empirical

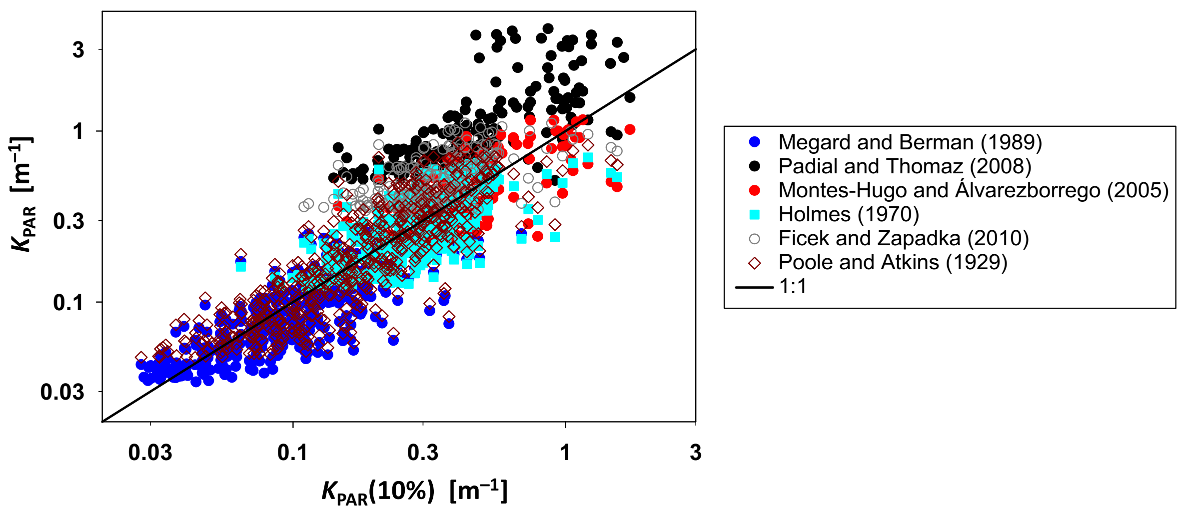

Fig. 7. As Fig. 3, but Z_{SD} estimated with the classical Secchi theory (those shown in Fig. 6) were used for the conversion to K_{PAR}.

relationships have been developed between Z_{SD} and Chl in the past decades (Berman et al. 1984; Lewis et al. 1988; Tilzer 1988; Falkowski and Wilson 1992; Fleming-Lehtinen and Laamanen 2012). However, because Z_{SD} is a measure of the bulk optical property, while Chl is just one of the components to affect waters' optical properties and then Z_{SD}, it is no surprise to see a wide range of variations in the relationship between Z_{SD} and Chl, so here we omit a comparison of the regional- or data-specific relationships. Rather, for Case-1 waters where at least conceptually Chl is the primary or only factor in modulating the optical properties of a water body (Morel 1988; Morel and Maritorena 2001), it is valid to compare the relationships between observations and theoretical predictions.

Based on extensive measurements, Morel and Maritorena (2001) have developed a robust relationship between K_d and Chl that represents an average dependence of global oceans between the two,

$$K_d(\lambda) = K_w(\lambda) + \chi(\lambda)(\mathrm{Chl})^{e(\lambda)}. \tag{15}$$

Here, K_w, χ, and e are empirical coefficients derived from a large number of concurrent measurements of K_d and Chl in a wide range of environments, with a spectral range of 400–800 nm, 5-nm step (table 2 of Morel and Maritorena 2001).

From this relationship, as in Morel et al. (2007*a*), we are then able to generate K_d for a given set of Chl, and subsequently Z_{SD} of each Chl based on Eq. 4. We here set a Chl range of 0.01–30 mg/m^3 with a step of 20% increase (resulting in a total of 45 Chl values), and the resulting Z_{SD} for these Chl values are shown in Fig. 8 (the green dots). Because of the Case-1 nature, there is an excellent dependence ($R^2 > 0.99$) between Chl and Z_{SD} for this dataset, and this dependence can be modeled as a power function

$$\mathrm{Chl} = \frac{293.9}{(Z_{SD})^{2.345}}. \tag{16}$$

Also included in Fig. 8 is the relationship developed by Boyce et al. (2012) based on hundreds of thousands of global measurements of Chl and Z_{SD}, where the empirical dependence between the two properties is

$$\mathrm{Chl} = \frac{143.29}{(Z_{SD})^{2.08}}. \tag{17}$$

Although the empirical coefficients between the two relationships are quite different, the two dependencies show excellent agreement (*see* Fig. 8). For Chl in a range of 0.02–10 mg/m^3, the average percent difference for Chl estimated from Z_{SD} between Eq. 16 and Eq. 17 is ~ 20%. The difference

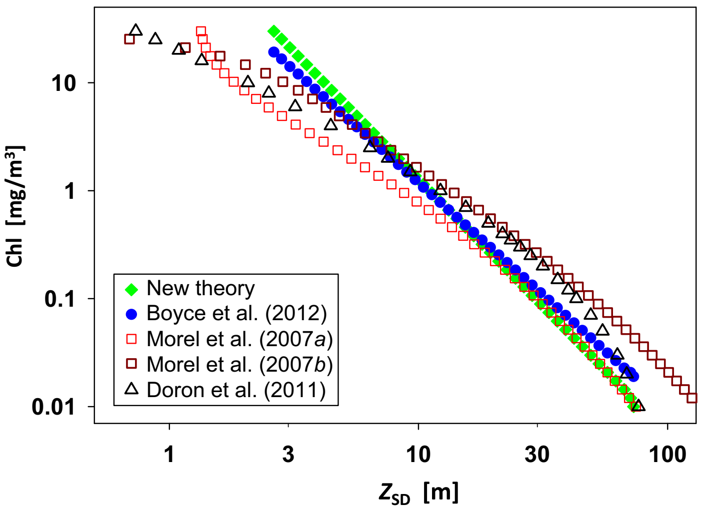

Fig. 8. A scatterplot between Z_{SD} and Chl for Case-1 waters obtained from numerical simulations, along with a relationship for global waters obtained from hundreds of thousands of measurements.

is larger (> 40%) for Chl less than ~ 0.03 mg/m^3 and for Chl greater than ~ 10 mg/m^3 (greater than ~ 30%). This is likely due to few accurate measurements for Chl < 0.03 mg/m^3 in historical datasets. On the other hand, higher Chl is usually associated with more turbid coastal waters, so there could be more factors contributing to varying Z_{SD} than Chl alone. Nevertheless, the excellent agreement for Chl in a range of ~ 0.03–10 mg/m^3 provides a strong theoretical base for both Eq. 16 and Eq. 17, which serves as another verification of the new theory and model regarding Z_{SD}. Note that the two models were developed completely independent of each other.

There were also attempts (Morel et al. 2007*a*) to model Z_{SD} of Case-1 waters based on the classical Z_{SD} model, with results as

$$Z_{SD-\Gamma=5.5} = 8.5 - 12.6\ Y + 7.36\ Y^2 - 1.43\ Y^3, \tag{18}$$

$$Z_{SD-\Gamma=8.7} = 13.5 - 19.6\ Y + 12.8\ Y^2 - 3.8\ Y^3, \tag{19}$$

with Y for $\mathrm{Log_{10}(Chl)}$. Morel et al. (2007*a*) argued that a Γ value of 5.5 (Morel 2007*a* in Fig. 8) is more reasonable for the global oceans, rather than the 8.7 (Morel 2007*b* in Fig. 8) suggested by Tyler (1968). Figure 8 includes the dependences of Z_{SD} vs. Chl of the two relationships above. It is noticed that the estimated Chl from $Z_{SD-\Gamma=5.5}$ matches very well with that estimated by Eq. 16 for Chl ~ 0.01–0.5 mg/m^3 (Z_{SD} ~ 20–70 m), but the estimated Chl (from $Z_{SD-\Gamma=5.5}$) would be significantly lower compared to that estimated by Eq. 16 and Eq. 17 for Chl greater than ~ 0.5 mg/m^3 (Z_{SD} less than ~ 10 m). If the relationship of $Z_{SD-\Gamma=8.7}$ is adopted, on the other hand, the estimated Chl would be two to three times greater than that estimated by Eqs. 16, 17 for Chl in the range of $\sim$ 0.01–1.0 mg/m^3, which usually happened for oceanic waters.

Another approach to estimate Z_{SD} of Case-1 waters based on the classical model is to follow the approximations of Doron et al. (2011), where a dynamic Γ as presented in Eq. 13 is adopted. As in, Morel and Maritorena (2001) and Morel et al. (2009), for a given Chl, $b_p(490)$ (particle scattering coefficient at 490 nm) and $b_{bp}(490)$ are calculated based on bio-optical models specifically developed for Case-1 waters (Loisel and Morel 1998; Loisel et al. 2007). Values of $a(490)$ and $R_w(490)$ are then derived from $K_d(490)$ and $b_{bp}(490)$ (*see* Morel et al. 2001), therefore $c(490)$ is obtained for a given Chl. With known $K_d(490)$, $R_w(490)$, and $c(490)$, Z_{SD} can then be estimated following the scheme of Doron et al. (2011), with resulted Chl vs. Z_{SD} also shown in Fig. 8 for the same set of Chl values. It is found that these estimates (termed as Z_{SD}_Doron) are between those of $Z_{SD-\Gamma=5.5}$ and $Z_{SD-\Gamma=8.7}$. Also, the Chl vs. Z_{SD}-Doron dependence does not match that of Boyce et al. (2012). These results echo the conclusion that the classical model for Z_{SD} is not consistent with the sighting of a Secchi disk in water.

An interesting finding is that for Chl = 0.01 mg/m^3, and based on the Case-1 bio-optical relationships, the predicted Z_{SD} is $\sim$ 73.0 m from Eq. 4. For the South Pacific Gyre (SPG) or "clearest" natural waters (Morel et al. 2007*b*), the measured $K_d(420)$ in November 2004 was $\sim$ 0.012 m^{-1} (Morel 2009), which suggests a $Z_{SD} \sim 80$ m following Eq. 5. Further, the concurrent Z_{SD} value in SPG was $\sim$ 73 m (Marlon Lewis, pers. comm.). These values suggest a maximum Z_{SD} of $\sim$ 75 m and a minimum Chl of $\sim$ 0.01 mg/m^3 for such "clearest" natural waters, although sample measurements of Chl showed a value of 0.02 mg/m^3 for the SPG during November 2014 (Morel 2009). This measured Chl is still under debate, as it suggests a much larger a_{ph} and K_d from the Case-1 bio-optical models (Morel and Maritorena 2001) compared to the measured values. The measurement and analyses of K_d and Z_{SD} rather supports a Chl value of $\sim$ 0.01 mg/m^3, unless significantly different bio-optical relationships exist for these waters (Morel et al. 2007*b*; Bricaud et al. 2010).

Z_{SD} vs. *Zeu*

Based on the above evaluations of the new Z_{SD} model from multiple perspectives as well as the verification presented in Lee et al. (2015*a*), it can be confidently concluded that the Z_{SD} model (Eqs. 4, 5) based on the new Secchi-disk theory successfully describes the dependence of Z_{SD} on waters' optical properties. Therefore, the Z_{SD} values from Eqs. 4 and 5 for the synthesized IOPs can be viewed as accurate numerical simulations for varying IOPs. Note that from Hydrolight simulations *Zeu* can also be determined directly from the simulated profiles of solar radiation. Thus, a set of theoretical Z_{SD} and *Zeu* for this Non-Case-1 dataset was obtained. It is found that the two are extremely linearly correlated ($R^2 > 0.99$) for this dataset, with the β value of Eq. 2 in a range of $\sim$ 3.1–4.0 (3.55 ± 0.15). Such a result provides strong support for the relationship observed from field measurements. The reported range of β in the literature is $\sim$ 1–10 though (Luhtala and Tolvanen 2013). Further, different values for clear and turbid waters were proposed (Holmes 1970; Smith 1979; Koenings and Edmundson 1991), with a consensus average β of $\sim$ 2.4 for clear waters (Smith 1979; Koenings and Edmundson 1991). Again, this puzzle and inconsistency regarding the variation of β values is primarily due to the ambiguity of K_{PAR}. This is because *Zeu* in historical studies (Koenings and Edmundson 1991) was derived from

$$Zeu = \frac{4.6}{K_{PAR}}, \tag{20}$$

with K_{PAR} further determined generally from measurements of PAR profiles in the surface layer rather than actually between the surface and *Zeu*. As discussed in detail in "Z_{SD} vs. K_{PAR} section," there are various uncertainties associated with each individual K_{PAR} determined from field measurements. Consequently, a wide range of *Zeu*/Z_{SD} ratios could be found from in situ data. Further, surface K_{PAR} is in general larger than K_{PAR}(0-*Zeu*), thus the calculated *Zeu,* following Eq. 20 by assuming a vertically constant K_{PAR}, will result in shallower *Zeu*, subsequently a smaller β value would be derived. Also, because there is a much larger depth variation of K_{PAR} for clear waters (*see* Fig. 5), there will be a trend of smaller β values from field measurements for clearer waters than that for more turbid waters, as indicated in Holmes (1970) and Luhtala and Tolvanen (2013). For more turbid waters where K_{PAR} is generally less depth-varying (*see* Fig. 5), Holmes (1970) suggested a β value of 3.5 is more appropriate. This value is in remarkable agreement with that found from the numerical simulations here. On the other hand, a value of 2.0 for clearer waters suggested by Holmes (1970) would significantly underestimate *Zeu*. This value of 2.0 is basically a result of mistakenly assuming vertically constant K_{PAR} while at the same time using K_{PAR} of the surface layer to represent K_{PAR} of the euphotic zone. Another likely source of smaller β of oceanic waters is the impact of subsurface Chl maximum, which is much deeper than Z_{SD}, but could be above *Zeu* and then results in shallower *Zeu* than that of homogeneous waters. However, such a scenario is not common, because many observations also showed that *Zeu* were shallower than the depth of Chl maximum (Banse 2004; Marra et al. 2014).

The above comparison suggests that *Zeu* estimated from Z_{SD} with an averaged consensus β value of 2.4 (at least for clear waters) will be underestimated by $\sim$ 33%. Thus, at least for homogeneous waters in the upper water column, it is important to use the new β value for this conversation. Further, because β is nearly a constant (within $\sim$ 3% variation) for the wide range of synthetic IOPs, it indicates the estimated *Zeu* from field measured Z_{SD} will be with an uncertainty under ∼ 15% for most natural waters, which is the uncertainty in present field-measured Z_{SD}, as long as the water type is common and the water column is not stratified. Such accuracy will have profound value and impact in applying the century-long Z_{SD} values for oceanographic studies.

Light level at Z_{SD}

It is also of interest to know the light level (percent of light at surface) at the Secchi-disk depth, and historical measurements reported values in a range of 5–40%, with an average as ∼ 18% (Koenings and Edmundson 1991). However, based on the classical theory, the predicted light level is ∼ 10% (Preisendorfer 1986), another gap regarding Secchi theory vs. measurements. As this light level is quantified as the ratio of PAR(Z_{SD}) to PAR(0), it can be calculated as

$$T_{SD} = \exp\left(-K_{PAR}(Z_{SD}) \times Z_{SD}\right). \tag{21}$$

We may thus estimate T_{SD} for the simulated data. Because K_{PAR} is not consistent vertically (*see* Fig. 5), it is critical to take the vertical variation of K_{PAR} into consideration for this estimation. For such, Lee et al. (2005*a*) developed a $K_{PAR}(z)$ model based on Hydrolight simulations as

$$K_{PAR}(z) = K_1 + \frac{K_2}{(1+z)^{0.5}}, \tag{22}$$

with K_1 and K_2 functions of $a(490)$ and $b_b(490)$ as well as solar zenith angle. Thus, because $a(490)$ and $b_b(490)$ are given for the synthesized data, while Z_{SD} is derived following Eq. 4 after Hydrolight simulations, it is straightforward to calculate T_{SD} from Eqs. 21, 22. It is found that T_{SD} of this simulated dataset is in a range of 0.12–0.24 (0.18 ± 0.03), which is remarkably consistent with the range (∼ 10–25%) reported in Beeton (1958). The average value of 0.18 (along with a very small deviation) is "identical" to that reported in Poole and Atkins (1929), and consistent with the average in Koenings and Edmundson (1991), but slightly lower than the ∼ 22% reported in Megard and Berman (1989). Note that the slightly higher T_{SD} value in Megard and Berman (1989) is due to the use of K_{PAR} from a deeper depth range, which is appropriate for the relationship with Z_{SD} (which is determined by the transparent window), but not appropriate for use of PAR attenuation, where the attenuation of all photons in the 400–700 nm range should be considered. The above reported averages of T_{SD} are much higher than the ∼ 9% reported in Aas et al. (2014) though, and it is not clear yet why the average T_{SD} value in Aas et al. (2014) is just about half of that reported in Poole and Atkins (1929) and Megard and Berman (1989). Nevertheless, the consistency in T_{SD} obtained between the new model prediction and a majority of earlier reported values from field measurements provides another support for the new Z_{SD} theory and model.

Conclusions

It was pointed out recently by Lee et al. (2015*a*) that the classical theory and model for Secchi depth have mistakes or shortcomings. The mismatch between the classical model and century-long observations is further revealed here with data from numerical simulations for both Case-1 and Non-Case-1 waters. On the other hand, the Z_{SD} model based on an innovative theory for Secchi-disk sighting shows remarkable agreements with both data and relationships published in the past ∼ 90 yr, regardless of water types. It can thus be confidently concluded that all the observed relationships between Z_{SD} and K_{PAR} in the past ∼ 90 yr can be unified under the new theoretically based Z_{SD} model. This relationship can then be used to provide a reliable and independent way to estimate K_{PAR}(10%) from the measurement of Z_{SD} in the field. In the meantime, the results emphasize that, contrary to historical practices or perceptions, it is not supported by the Secchi theory to estimate the beam attenuation coefficient from Secchi depth. All relationships developed between *c* and Z_{SD} are empirical in nature, as there is no such a relationship for global waters.

Further, it is found that the century-long puzzles associated the empirical coefficients between Z_{SD} and K_{PAR} and between Z_{SD} and *Zeu* in the literature can be well resolved with the depth-and-water-property-dependent characteristics of K_{PAR}. Fundamentally, because solar radiation changes color with increasing depth, and because K_{PAR} by definition is a measure of the attenuation of all photons in the visible domain, K_{PAR} of the surface layer in general cannot be used to represent K_{PAR} of the water column (between 0 and Z_{SD} or between 0 and *Zeu*). But this nature of K_{PAR} has been in general overlooked in the studies of Z_{SD} in the past decades. Because of such characteristics, K_{PAR} calculated from different groups could be very different even for the same water body if the range of depths used is not the same.

With the new model for Z_{SD} and simulations by Hydrolight for a wide range of water properties, it is found that there is an excellent ($R^2 > 0.99$) linear relationship between the *Zeu* and Z_{SD}, which is in agreement with observations in the past decades. However, the scaling constant to convert Z_{SD} to *Zeu* is 3.55 (± 0.15), rather than the 2.4 considered for homogeneous oceanic waters. This indicates that the euphotic zone depth was likely underestimated by ∼ 33% in the past when it was converted from Z_{SD} with 2.4 as the scaling factor. Further, after considering a vertically varying K_{PAR}, it is found that the light level at Z_{SD} is about 18% of PAR(0), which is in excellent agreement with field measurements.

Furthermore, it is found that the average dependence (or the so-called Case-1 waters) between Z_{SD} and Chl obtained from the new model is in excellent agreement with that developed purely from a wide range of global measurements. Thus, it supports the practice of converting historical Z_{SD} data to Chl, although just for averages, for the study of phytoplankton trends in the global oceans.

In view of the above, it is advised that it is time to cease using the classical Z_{SD} model for interpretation of Z_{SD} data or for its remote sensing from ocean color. Further, contrary to conclusions made $\sim$ 30 yr ago, the results here highlight the remarkable value of Z_{SD} data for accurately estimating K_{PAR}(10%) and *Zeu* for most natural waters, as long as the upper water column is not stratified or the constituents in water are not abnormal. Nevertheless, it is necessary to keep in mind that fundamentally Z_{SD} is determined by K_d in the transparent window of a water body.

References

Aas, E., J. Høkedal, and K. Sørensen. 2014. Secchi depth in the Oslofjord–Skagerrak area: Theory, experiments and relationships to other quantities. Ocean Sci. **10**: 177–199. doi:10.5194/os-10-177-2014

Banse, K. 2004. Should we continue to use the 1% light depth convention for estimating the compensation depth of phytoplankton for another 70 years. Limnol. Oceanogr. Bull. **13**: 49–52.

Bartleson, C. J., and E. J. Breneman. 1967. Brightness perception in complex fields. J. Opt. Soc. Am. **57**: 953–957. doi:10.1364/JOSA.57.000953

Beeton, A. M. 1958. Relationship between Secchi disc readings and light penetration in Lake Huron. Trans. Am. Fish. Soc. **87**: 73–79. doi:10.1577/1548-8659(1957)87[73:RBSDRA]2.0.CO;2

Behrenfeld, M. J., and P. G. Falkowski. 1997*a*. A consumer's guide to phytoplankton primary productivity models. Limnol. Oceanogr. **42**: 1479–1491. doi:10.4319/lo.1997.42.7.1479

Behrenfeld, M. J., and P. G. Falkowski. 1997*b*. Photosynthetic rates derived from satellite-based chlorophyll concentration. Limnol. Oceanogr. **42**: 1–20. doi:10.4319/lo.1997.42.1.0001

Berman, T., D. W. Townsend, S. Z. E. Sayed, C. C. Trees, and Y. Azov. 1984. Optical transparency, chlorophyll and primary productivity in the Eastern Mediterranean near the Israeli coast. Oceanol. Acta **1**: 367–372.

Binding, C. E., J. H. Jerome, R. P. Bukata, and W. G. Booty. 2007. Trends in water clarity of the lower great lakes from remotely sensed aquatic color. J. Great Lakes Res. **33**: 828–841. doi:10.3394/0380-1330(2007)33[828:TIWCOT]2.0.CO;2

Blackwell, H. R. 1946. Contrast thresholds of the human eye. J. Opt. Soc. Am. **36**: 624–643. doi:10.1364/JOSA.36.000624

Boivin, L. P., W. F. Davidson, R. S. Storey, D. Sinclair, and E. D. Earle. 1986. Determination of the attenuation coefficients of visible and ultraviolet radiation in heavy water. Appl. Opt. **25**: 877–882. doi:10.1364/AO.25.000877

Boyce, D. G., M. R. Lewis, and B. Worm. 2010. Global phytoplankton decline over the past century. Nature **466**: 591–596. doi:10.1038/nature09268

Boyce, D. G., M. Lewis, and B. Worm. 2012. Integrating global chlorophyll data from 1890 to 2010. Limnol. Oceanogr.: Methods **10**: 840–852. doi:10.4319/lom.2012.10.840

Boyce, D. G., M. Dowd, M. R. Lewis, and B. Worm. 2014. Estimating global chlorophyll changes over the past century. Prog. Oceanogr. **122**: 163–173. doi:10.1016/j.pocean.2014.01.004

Boyce, D. G., and B. Worm. 2015. Patterns and ecological implications of historical marine phytoplankton change. Mar. Ecol. Prog. Ser. **534**: 251–272. doi:10.3354/meps11411

Bracchini, L., A. M. Dattilo, V. Hull, S. A. Loiselle, A. Tognazzi, and C. Rossi. 2009. Modelling Upwelling irradiance using Secchi disk depth in lake ecosystems. J. Limnol. **68**: 83–91. doi:10.4081/jlimnol.2009.83

Bricaud, A., M. Babin, H. Claustre, J. Ras, and F. Tieche. 2010. Light absorption properties and absorption budget of Southeast Pacific waters. J. Geophys. Res. Oceans **115**: C08009. doi: 08010.01029/02009JC005517

Bukata, R. P., J. H. Jerome, and J. E. Bruton. 1988. Relationships among Secchi disk depth, beam attenuation coefficient, and irradiance attenuation coefficient for Great Lakes waters. J. Great Lakes Res. **14**: 347–355. doi:10.1016/S0380-1330(88)71564-6

Carlson, R. E. 1977. A trophic state index for lakes. Limnol. Oceanogr. **22**: 361–369. doi:10.4319/lo.1977.22.2.0361

Davies-Colley, R. J., and W. N. Vant. 1988. Estimation of optical properties of water from Secchi disk depths. Water Res. Bull. **24**: 1329–1335. doi:10.1111/j.1752-1688.1988.tb03054.x

Doron, M., M. Babin, O. Hembise, A. Mangin, and P. Garnesson. 2011. Ocean transparency from space: Validation of algorithms using MERIS, MODIS and SeaWiFS data. Remote Sens. Environ. **115**: 2986–3001. doi:10.1016/j.rse.2011.05.019

Doron, M., M. Babin, A. Mangin, and O. Hembise. 2007. Estimation of light penetration, and horizontal and vertical visibility in oceanic and coastal waters from surface reflectance. J. Geophys. Res. **112**: C06003. doi:06010.01029/02006JC004007

Duntley, S. Q. 1952. The visibility of submerged objects, p. 74. Visibility Lab.

Effler, S. W., and others. 2017. A mechanistic model for Secchi disk depth, driven by light scattering constituents. Water Air Soil Poll. **228**: 153. doi:10.1007/s11270-017-3323-7

Falkowski, P. G. 1998. Using satellite data to derive primary productivity in the world ocean. *In* S. B. Hooker and E. R. Firestone [eds.], SeaWiFS technical report series. NASA.

Falkowski, P. G., and C. Wilson. 1992. Phytoplankton productivity in the North Pacific Ocean since 1900 and implications for absorption of anthropogenic CO_2. Nature **358**: 741–743. doi:10.1038/358741a0

Ficek, D., and T. Zapadka. 2010. Variability of bio-optical parameters in Lake Jasień Północny and Lake Jasień Południowy. Limnol. Rev. **10**: 67–76. doi:10.2478/v10194-011-0008-2

Fleming-Lehtinen, V., and M. Laamanen. 2012. Long-term changes in Secchi depth and the role of phytoplankton in explaining light attenuation in the Baltic Sea. Estuar. Coast. Shelf Sci. **102–103**: 1–10. doi:10.1016/j.ecss.2012.02.015

Fournier, G. R., and J. L. Forand. 1994. Analytic phase function for ocean water, p. 194–201. *In* J. Jaffe [ed.], Ocean optics XII. SPIE.

Freeman, R. B. 1967. Contrast interpretation of brightness constancy. Psychol. Bull. **67**: 165–187. doi:10.1037/h0024256

Gallegos, C., D. Correll, and J. Pierce. 1990. Modeling spectral diffuse attenuation, absorption, and scattering coefficients in a turbid estuary. Limnol. Oceanogr. **35**: 1486–1502. doi:10.4319/lo.1990.35.7.1486

Gallegos, C. L., P. J. Werdell, and C. R. McClain. 2011. Long-term changes in light scattering in Chesapeake Bay inferred from Secchi depth, light attenuation, and remote sensing measurements. J. Geophys. Res. **116**: C00H08. doi:10.1029/2011JC007160

Gordon, H. R., and A. W. Wouters. 1978. Some relationships between Secchi depth and inherent optical properties of natural waters. Appl. Opt. **17**: 3341–3343. doi:10.1364/AO.17.003341

Gordon, H. R., and A. W. Wouters. 1985. Ship perturbation of irradiance measurements at sea, 1: Monte Carlo simulations. Appl. Opt. **24**: 4172–4182. doi:10.1364/AO.24.004172

Gordon, H. R., and A. W. Wouters. 1989. Can the Lambert-Beer law be applied to the diffuse attenuation coefficient of ocean water? Limnol. Oceanogr. **34**: 1389–1409. doi:10.4319/lo.1989.34.8.1389

Graham, J. 1966. Secchi disc observations and extinction coefficients in the central and eastern North Pacific Ocean. Limnol. Oceanogr. **11**: 184–190. doi:10.4319/lo.1966.11.2.0184

Gregg, W. W., and K. L. Carder. 1990. A simple spectral solar irradiance model for cloudless maritime atmospheres. Limnol. Oceanogr. **35**: 1657–1675. doi:10.4319/lo.1990.35.8.1657

He, X., and others. 2017. Recent changes of global ocean transparency observed by SeaWiFS. Cont. Shelf Res. **143**: 159–166. doi:10.1016/j.csr.2016.09.011

Holmes, R. W. 1970. The Secchi disk in turbid coastal waters. Limnol. Oceanogr. **15**: 688–694. doi:10.4319/lo.1970.15.5.0688

Hou, W., Z.-P. Lee, and A. D. Weidemann. 2007. Why does the Secchi disk disappear? An imaging perspective. Opt. Express. **15**: 2791–2802. doi:10.1364/OE.15.002791

Idso, S. B., and R. G. Gilbert. 1974. On the universality of the Poole and Atkins Secchi disk-light extinction equation. J. Appl. Ecol. **11**: 399–401. doi:10.2307/2402029

IOCCG-OCAG. 2003. Model, parameters, and approaches that used to generate wide range of absorption and backscattering spectra. International Ocean Colour Coordinating Group. Available from http://www.ioccg.org/groups/OCAG_data.html

IOCCG. 2006. Remote sensing of inherent optical properties: Fundamentals, tests of algorithms, and applications, p. 126. *In* Z.-P. Lee [ed.], Reports of the international ocean-colour coordinating group, no. 5. IOCCG.

Kirk, J. T. O. 1994. Light & photosynthesis in aquatic ecosystems. Univ. Press.

Koenings, J. P., and J. A. Edmundson. 1991. Secchi disk and photometer estimates of light regimes in Alaskan lakes: Effects of yellow color and turbidity. Limnol. Oceanogr. **36**: 91–105. doi:10.4319/lo.1991.36.1.0091

Lee, Z. P. 2009. KPAR: An optical property associated with ambiguous values. J. Lake Sci. **21**: 159–164. doi:10.18307/2009.0202

Lee, Z. P., K. P. Du, and R. Arnone. 2005. A model for the diffuse attenuation coefficient of downwelling irradiance. J. Geophys. Res. **110**: C02016. doi: 1029/2004JC002275

Lee, Z. P., K. Du, R. Arnone, S. C. Liew, and B. Penta. 2005. Penetration of solar radiation in the upper ocean—A numerical model for oceanic and coastal waters. J. Geophys. Res. **110**: C09019. doi: 09010.01029/02004JC002780

Lee, Z. P., S. L. Shang, K. P. Du, J. Wei, and R. Arnone. 2014. Usable solar radiation and its attenuation in the upper water column. J. Geophys. Res. **119**: 1488. doi:10.1002/2013JC009507

Lee, Z., and others. 2015. Secchi disk depth: A new theory and mechanistic model for underwater visibility. Rem. Sens. Enviro. **169**: 139–149. doi:10.1016/j.rse.2015.08.002

Lee, Z., J. Wei, K. Voss, M. Lewis, A. Bricaud, and Y. Huot. 2015. Hyperspectral absorption coefficient of "pure" seawater in the range of 350–550 nm inverted from remote sensing reflectance. Appl. Opt. **54**: 546–558. doi:10.1364/AO.54.000546

Lee, Z., and others. 2017. Secchi disk observation with spectral-selective glasses in blue and green waters. Opt. Exp. **25**: 19878–19885. doi:10.1364/OE.25.019878

Levin, I. M., and T. M. Radomyslskaya. 2012. Estimate of water inherent optical properties from Secchi depth. Atmos. Oceanic Phys. **48**: 214–221. doi:10.1134/S0001433812020065

Lewis, M. R., N. Kuring, and C. Yentsch. 1988. Global patterns of ocean transparency: Implications for the new production of the open ocean. J. Geophys. Res. **93**: 6847–6856. doi:10.1029/JC093iC06p06847

Loisel, H., and A. Morel. 1998. Light scattering and chlorophyll concentration in Case 1 waters: A reexamination. Limnol. Oceanogr. **43**: 847–858. doi:10.4319/lo.1998.43.5.0847

Loisel, H., X. Meriaux, J. F. Berthon, and A. Poteau. 2007. Investigation of the optical backscattering to scattering ratio of marine particles in relation to their biogeochemical composition in the eastern English Channel and southern North Sea. Limnol. Oceanogr. **52**: 739–752. doi:10.4319/lo.2007.52.2.0739

Lugo-Fernández, A., M. Gravois, and T. Montgomery. 2008. Analysis of Secchi depths and light attenuation coefficients in the Louisiana-Texas shelf, northern Gulf of Mexico. Gulf Mexico Sci. **26**: 14–27.

Luhtala, H., and H. Tolvanen. 2013. Optimizing the use of Secchi depth as a proxy for euphotic depth in coastal waters: An empirical study from the Baltic Sea. ISPRS Int. J. Geo-Inf. **2**: 1153–1168. doi:10.3390/ijgi2041153

Marra, J. F., V. P. Lance, R. D. Vaillancourt, and B. R. Hargreaves. 2014. Resolving the ocean's euphotic zone. Deep Sea Res. I **83**: 45–50. doi:10.1016/j.dsr.2013.09.005

McCormick, N. J. 1995. Mathematical models for the mean cosine of irradiance and the diffuse attenuation coefficient. Limnol. Oceanogr. **40**: 1013–1018. doi:10.4319/lo.1995.40.5.1013

Megard, R. O., and T. Berman. 1989. Effects of algae on the Secchi transparency of the southeastern Mediterranean Sea. Limnol. Oceanogr. **34**: 1640–1655. doi:10.4319/lo.1989.34.8.1640

Middleton, W. E. K. 1957. Vision through the atmosphere, p. 254–287. *In* S. Flugge [ed.], Encyclopedia of physics: Geophysics II. Springer-Verlag.

Mishra, S., D. R. Mishra, Z.-P. Lee, and C. Tucker. 2013. Quantifying cyanobacterial phycocyanin concentration in turbid productive waters: A quasi-analytical approach. Remote. Sens. Envi. **133**: 141–151. doi:10.1016/j.rse.2013.02.004

Mobley, C. D. 1994. Light and water: radiative transfer in natural waters. Academic Press.

Mobley, C. D., and L. K. Sundman. 2013. HydroLight 5.2 user's guide. Sequoia Scientific.

Montes-Hugo, M. A., and S. Álvarezborrego. 2005. Empirical relations to estimate underwater PAR attenuation in San Quintín Bay using Secchi depth and horizontal sighting range. Ciencias Marinas **31**: 685–695. doi:10.7773/cm.v31i4.27

Morel, A. 1988. Optical modeling of the upper ocean in relation to its biogenous matter content (Case I waters). J. Geophys. Res. **93**: 10749–10768. doi:10.1029/JC093iC09p10749

Morel, A. 2009. Are the empirical relationships describing the bio-optical properties of case 1 waters consistent and internally compatible? J. Geophys. Res. **114**: C01016. doi:10.1029/2008JC004803

Morel, A., and S. Maritorena. 2001. Bio-optical properties of oceanic waters: A reappraisal. J. Geophys. Res. **106**: 7163–7180. doi:10.1029/2000JC000319

Morel, A., H. Claustre, D. Antoine, and B. Gentili. 2007*a*. Natural variability of bio-optical properties in Case 1 waters: Attenuation and reflectance within the visible and near-UV spectral domains, as observed in South Pacific and Mediterranean waters. Biogeosciences **4**: 913–925. doi:10.5194/bg-4-913-2007

Morel, A., and others. 2007*b*. Optical properties of the "clearest" natural waters. Limnol. Oceanogr. **52**: 217–229. doi:10.4319/lo.2007.52.1.0217

Olmanson, L. G., M. E. Bauer, and P. L. Brezonik. 2008. A 20-year Landsat water clarity census of Minnesota's 10,000 lakes. Remote Sens. Environ. **112**: 4086–4097. doi:10.1016/j.rse.2007.12.013

Padial, A. A., and S. M. Thomaz. 2008. Prediction of the light attenuation coefficient through the Secchi disk depth: Empirical modeling in two large Neotropical ecosystems. Limnology **9**: 143–151. doi:10.1007/s10201-008-0246-4

Petzold, T. J. 1972. Volume scattering functions for selected natural waters, p. 72–78. Scripps Institution of Oceanography.

Platt, T. 1986. Primary production of ocean water column as a function of surface light intensity: Algorithms for remote sensing. Deep-Sea Res. **33**: 149–163. doi:10.1016/0198-0149(86)90115-9

Platt, T., C. Caverhill, and S. Sathyendranath. 1991. Basin-scale estimates of oceanic primary production by remote sensing: The North Atlantic. J. Geophy. Res. **96**: 15147–15159. doi:10.1029/91JC01118

Poole, H. H., and W. R. G. Atkins. 1929. Photo-electric measurements of submarine illumination throughout the year. J. Mar. Biol. Assoc. UK **16**: 297–324. doi:10.1017/S0025315400029829

Pope, R., and E. Fry. 1997. Absorption spectrum (380–700 nm) of pure waters: II. Integrating cavity measurements. Appl. Opt. **36**: 8710–8723. doi:10.1364/AO.36.008710

Preisendorfer, R. W. 1986. Secchi disk science: Visual optics of natural waters. Limnol. Oceanogr. **31**: 909–926. doi:10.4319/lo.1986.31.5.0909]

Sathyendranath, S., and T. Platt. 1995. Remote sensing of water-column primary production, p. 236–243. *In* W. K. W. Li and Maestrini [eds.], Measurement of primary production from the molecular to the global scale. ICES Marine Science Symposia.

Secchi, P. A. 1864. Relazione delle esperienze fatte a bordo della pontificia pirocorvetta Imacolata Concezione per determinare la trasparenza del mare. Memoria del PA Secchi. Il Nuovo Cimento Giornale de Fisica, Chimica e Storia Naturale, Ottobre 1864, Published 1865 **20**: 205–237. (G. B. Paravia, Torino, 1864).

Shang, S., Z. Lee, L. Shi, G. Lin, G. Wei, and X. Li. 2016. Changes in water clarity of the Bohai Sea: Observations from MODIS. Remote Sens. Environ. **186**: 22–31. doi:10.1016/j.rse.2016.08.020

Smith, V. H. 1979. Nutrient dependence of primary productivity in lakes. Limnol. Oceanogr. **24**: 1051–1064. doi:10.4319/lo.1979.24.6.1051

Sogandares, F. M., and E. S. Fry. 1997. Absorption spectrum (340–640 nm) of pure water. I. Photothermal measurements. Appl. Opt. **36**: 8699–8709. doi:10.1364/AO.36.008699

Stramski, D., and L. Legendre. 1992. Laboratory simulation of light-focusing by water-surface waves. Mar. Biol. **114**: 341–348. doi:10.1007/BF00349537

Suresh, T., P. Naik, M. Bandishte, E. Desa, A. Mascaranahas, and S. G. P. Matondkar. 2006. Secchi depth analysis using bio-optical parameters measured in the Arabian Sea, p. 101–110. *In* R. J. Frouin, V. K. Agarwal, H. Kawamura, S. Nayak and D. Pan [eds.], Remote sensing of the marine environment. Proceedings of the SPIE.

Tilzer, M. M. 1988. Secchi disk—Chlorophyll relationships in a lake with highly variable phytoplankton biomass. Hydrobiologia **162**: 163–171. doi:10.1007/BF00014539

Tyler, J. E. 1968. The Secchi disc. Limnol. Oceanogr. **13**: 1–6. doi:10.4319/lo.1968.13.1.0001

Walker, T. A. 1980. A correction of the Poole and Atkins Secchi disc/light-attenuation formula. J. Mar. Biol. Ass. UK **60**: 769–771. doi:10.1017/S0025315400040431

Wei, J., M. R. Lewis, R. V. Dommelen, C. J. Zappa, and M. S. Twardowski. 2014. Wave-induced light field fluctuations in measured irradiance depth profiles: A wavelet analysis. J. Geophys. Res. **119**: 1344. doi:10.1002/2013JC009572

Weidemann, A. D., and T. T. Bannister. 1986. Absorption and scattering coefficients in lrondequoit Bay. Limnol. Oceanogr. **31**: 567–583. doi:10.4319/lo.1986.31.3.0567

Wernand, M. 2010. On the history of the Secchi disc. J. Eur. Opt. Soc. Rapid Publ. **5**: 10013s. doi:10.2971/jeos.2010.10013s

Zaneveld, J. R., and W. S. Pegau. 2003. Robust underwater visibility parameter. Opt. Exp. **11**: 2997–3009. doi:10.1364/OE.11.002997

Zhang, X., L. Hu, and M.-X. He. 2009. Scattering by pure seawater: Effect of salinity. Optics Express. **17**: 5698–5710. doi:10.1364/OE.17.005698

Zhang, Y., X. Liu, Y. Yin, M. Wang, and B. Qin. 2012. Predicting the light attenuation coefficient through Secchi disk depth and beam attenuation coefficient in a large, shallow, freshwater lake. Hydrobiologia **693**: 29–37. doi:10.1007/s10750-012-1084-2

Acknowledgements

Financial support from the Chinese Ministry of Science and Technology (#2016YFC1400905, #2016YFA0601201, Shang), the National Aeronautics and Space Administration (NASA) Ocean Biology and Biogeochemistry and Water and Energy Cycle Programs (NNX14AQ47A, NNX14AM15G, NNX15AC84G, Lee), National Oceanic and Atmospheric Administration (NOAA) JPSS VIIRS Ocean Color Cal/Val Project (NA11OAR4320199, Lee), and the University of Massachusetts Boston is greatly appreciated. We thank Mr. Charles Kovach for proofreading this manuscript.

Conflict of Interest

None declared.

Submitted 27 December 2017
Revised 02 April 2018
Accepted 25 April 2018

Associate editor: David Antoine